crystals

MDPI

Article

Kinetic Phase Behavior of Binary Mixtures of Tri-Saturated Triacylglycerols Containing Lauric Acid

Sabine Danthine

Food Technology, Gembloux Agro Bio Tech, Liège University, 5030 Gembloux, Belgium; sabine.danthine@uliege.be

Abstract: Describing fat phase behavior is of significant interest for food and non-food applications. One recognized approach to understand the behavior of complex fatty systems is to simplify the fat matrix and to emphasize only the main triacylglycerol (TAG) components. In this context, the kinetic phase behavior and phase transformation paths of binary mixtures of selected saturated monoacids (trilaurin (LaLaLa), trimyristin (MMM), and tripalmitin (PPP)) and of mixed saturated triacylglycerols containing lauric (La) and myristic (M) acids (MMLa and LaLaM) typical from lauric fats were investigated. Kinetic phase diagrams were constructed based on DSC heating thermograms (fast cooling and reheating at 5 °C min^{-1}) and powder X-ray diffraction data. The investigated binary kinetic phase diagram presented an apparently typical eutectic behavior, with a eutectic point that varies depending on the blend composition. Introducing mixed saturated TAGs (MMLa or LaLaM) in binary blends led to a shift in the position of the eutectic point. Considering the binary blends made of LaLaLa, it was shifted from X_{LaLaLa} = 0.7 in the LaLaLa–MMM system to X_{LaLaLa} = 0.5 for the LaLaLa–MMLa mixture, and to X_{LaLaLa} = 0.25 for the LaLaLa–LaLaM blend. Finally, the blend made of the two mixed TAGs (MMLa–LaLaM) also presented a complex non-ideal behavior.

Keywords: lauric fat; polymorphism; phase behavior diagram; crystallization

Citation: Danthine, S. Kinetic Phase Behavior of Binary Mixtures of Tri-Saturated Triacylglycerols Containing Lauric Acid. *Crystals* **2024**, *14*, 807. https://doi.org/10.3390/cryst14090807

Academic Editor: Petros Koutsoukos

Received: 17 July 2024
Revised: 23 August 2024
Accepted: 29 August 2024
Published: 12 September 2024

1. Introduction

The melting and polymorphic behaviors of a fat are of great importance in the physical and sensory attributes of fatty products such as chocolate, margarines, creams, and suppositories. They can impact the functionality and the shelf life of the final product due to polymorphic transformations [1]. The characterization of the melting and crystallization behavior of fats is then highly useful for the development of new fat-based products and/or the improvement of existing products. Among all the vegetable oils and fats, lauric fats are commonly used in the food industry [2]. Palm kernel oil (PKO), which is extracted from the kernel of palm fruits and is characterized by a high amount of lauric acid (La) (48%) and myristic acid (M) (16%) [3], and coconut oil (CO), which is also characterized by a high amount of La (43%) and M (21%) [4], are the most frequently used lauric fats in the food industry [5]. Other minor lauric fats also exist; for example, *Irvingia gabonensis* fat (IG), which contains mainly M (50%) and La (37%) acids [1], and black soldier fly (BSF) larvae oil that contains about 30% of La, 12.5% M, and 16.5% of palmitic (P) acids [6].

Coconut oil has possible health benefits linked to its high amount of medium-chain fatty acids, as they are used rapidly by the body compared to long-chain fatty acids (FA). In this way, they are not stored in adipose body tissues [7–9]. Coconut oil is commonly used in the food sector to produce several confectionery products such as coatings and fillings. PKO also contains oleic (O) acid (15%) and is sometimes hydrogenated. PKO and hydrogenated PKO (HPKO) are also widely used in the food industry, particularly for producing shortenings, margarines, whipping non-dairy creams, and cocoa butter substitutes. Lauric fats are used for producing cocoa butter substitutes (CBSs), which are used to enrobe biscuits or bakery products instead of chocolate. Studies have been

conducted regarding the crystallization behavior of such lauric fats both in bulk [10–14] and emulsified systems [15–20]. Anhiouvi et al. [2] demonstrated that the melting and crystallization characteristics of different lauric fats, even those belonging to the same type, were strongly dependent on their triacylglycerol (TAG) composition; they highlighted that the proportion of medium-chain FAs to long-chain FAs seemed to determine the variant of existing β′-crystals.

Describing fat phase behavior (transitions between the solid and liquid phase, polymorphism of the solid state, and the transitions between solid states) is of significant interest across various food and non-food application areas [21], and it is now well recognized that investigating the phase behavior of TAG blends is of great importance for food, cosmetic, and pharmaceutical products [22]. A deep understanding is highly relevant because the fat structures, which depend on the polymorphic occurrence and mixing behavior of the TAG they contain, largely influence the macroscopic properties of the product, such as texture, plasticity, and mouthfeel. The TAG composition of natural fats is often highly heterogeneous; they are blends of saturated monoacids, saturated mixed acid types, and/or saturated–unsaturated mixed type TAGs. One recognized approach to understand the behavior of complex real-world fatty systems is to simplify the fat matrix and to emphasize only their main TAG components [21]. Investigating a reduced number of TAG components in binary or ternary systems has been shown to deliver several relevant pieces of information to understand the behavior of real-world fat systems [23]. Saturated monoacid triacylglycerols (StStSt) such as trilaurin (LaLaLa), trimyristin (MMM), and tripalmitin (PPP) have the simplest chemical shape, and they can serve as TAG models. Understanding the polymorphism of mixed-acid saturated TAGs such as LaLaM and MMLa is, however, of significance. Indeed, in the case of lauric fats, La- and M-containing triacylglycerols are among the main components that deserve to be investigated. The sum of LaLaLa + LaLaM + MMLa represents about 38% of the TAGs found in PKO [3]. The same three TAGs represent about 50% of the TAG composition of coconut oil [4], more than 50% of IG and about 40% of BSF larvae oil.

To understand the crystallization behavior of lauric fats, it is therefore relevant to study the behavior of these three TAGs in a mixture, but also in combination with other tri-saturated TAGs that are part of the composition of these particular fats.

Three basic polymorphic forms have been described for lipids—α, β′, and β—with a polymorphism of the monotectic type. The intermediate forms (metastable) transform into more stable forms through solid-state or melt-mediated transitions.

Several phase behavior diagrams have already been reported in the literature, and the paper of Machridachis-Gonzales et al. [23] provides a review on the relevant papers published over a few decades presenting binary and ternary diagrams. More specifically, regarding saturated TAG mixtures, some of them have been investigated by different groups [22,24,25], but much remains to be investigated. Up to now, limited data are available in the literature comparing the thermal and structural behavior of tri-saturated TAGs containing lauric acid. A comparative study of binary systems including the main TAGs of lauric fats (LaLaLa, MMLa, and LaLaM), which are all obtained under similar conditions, is still missing. Moreover, the polymorphic behavior of MMLa and LaLaM has not yet been reported in the literature.

In this context, the work reported here aims to establish this basic information regarding lauric fats by constructing binary phase behavior diagrams of tri-saturated TAGs. The work reported here systematically explores and compares these phase diagrams obtained in the same thermal conditions, thanks to DSC combined with variable temperature powder XRD.

The results of this study allow clarification of the phenomena observed during the crystallization of different lauric fats. The results are useful for the food industry as they can help in understanding the functionality of lauric fat-based fatty products and in developing products for specific food applications based on such fats.

2. Materials and Methods

2.1. Materials

Trilaurin (LaLaLa), trimyristin (MMM), tripalmitin (PPP), 1,2-Laurin 3-Myristin (LaLaM), and 1,2 Myristin 3 Laurin (MMLa) were purchased from Larodan (Solna, Sweden). Purity, verified using gas–liquid chromatography (GLC), was above 99%. Samples were used as received, without any further purification. The binary mixtures were prepared by accurately weighting the pure TAGs to reach the right proportion, then melting the mixture at 80 °C and mixing for several minutes using a vortex mixer to ensure homogeneity. The blends were prepared at 0.1 increments from 0 to 1.0 proportions by weight. For some blends, 0.75/0.25 and 0.25/0.75 proportions were also examined. Samples were kept in sealed vials at −20 °C until use.

2.2. Methods

2.2.1. Differential Scanning Calorimetry (DSC)

The DSC cooling and melting profiles of all the studied blends were obtained using a Q1000 DSC (TA Instruments, New Castle, DE, USA) connected to a refrigerated cooling system (TA Instruments, New Castle, DE, USA). Samples were directly weighted in aluminum hermetic pans (TA Instruments, New Castle, DE, USA). Calibration (melting temperature, T_m °C; enthalpy, ΔH, $J \cdot g^{-1}$) was made with indium (melting point 156.6 °C) and n-dodecane (melting point 9.56 °C) standards; nitrogen was used as the purge gas in order to prevent condensation in the cells.

To investigate the polymorphic mixing behavior of the different blends under metastable conditions, the thermal treatment was applied as follows:

Samples were first heated up to 80 °C to ensure the complete melting and erasing of the thermal memory. After 10 min at this temperature, they were quickly frozen from the melt up to −60 °C, at −25 $°C \cdot min^{-1}$; they were then kept at this temperature for 10 min in order to ensure complete solidification. Melting profiles were then registered from −60 °C to 80 °C at a heating rate of 5 $°C \cdot min^{-1}$. Temperatures of endotherms and exotherms were registered at the maximum of the peaks (T_{peak}, melting and transitions). All samples were analyzed in triplicate.

2.2.2. Powder X-ray Diffractometry (PXRD)

Polymorphism was investigated using powder X-ray diffraction using a D8 Advance diffractometer (Bruker, Germany) equipped with an X-ray generator Kristalloflex K780 (Bruker, Karlsruhe, Germany) (λ Cu = 1.54178 A, 40 kW, 30 mA), and a Vantec-1 detector (Bruker, Karlsruhe, Germany) and a Lynxeye Detector (Bruker, Karlsruhe, Germany). Temperature control was performed with a TTK 450 Anton Paar system connected to a TCU-100 control Unit (Anton Paar, Graz, Austria), which was connected to a water bath. A flat aluminum sample holder was used. Samples were first fully melted to erase previous crystal memory; afterwards, thermal conditioning was identical as for DSC measurements. Short (15–27° 2θ) and long (1–15° 2θ) spacing regions were analyzed in separate runs. Silver behenate and pure stable β-tristearin were used to calibrate the SAXS and WAXS regions, respectively.

The phase diagrams of the TGA mixtures were constructed using the melting and transformation temperatures determined with DCS (i.e., using the endo and exo peak maxima) combined with XRD data (i.e., when the SAXS/WAXS diffraction patterns changed); the polymorphic structures were identified using the WAXS data. The diffraction patterns were analyzed with EVA Diffrac.suite V4.2.2. software (Bruker, Karlsruhe, Germany).

3. Results

3.1. Polymorphism and Melting Behavior of Pure TAGs (Melting, Quenching, and Reheating at 5 °C min^{-1})

The pure triacylglycerols were first investigated under dynamic conditions; the DSC melting profiles are presented in Figure 1.

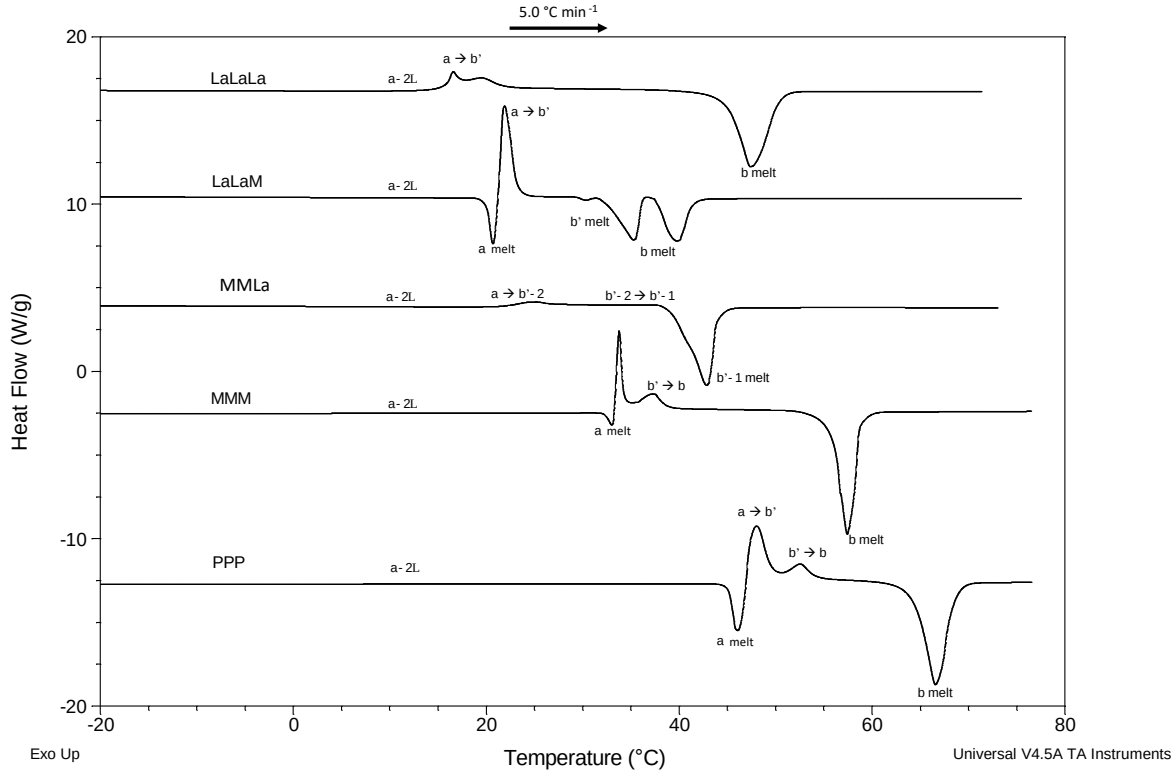

Figure 1. DSC melting thermograms of the investigated tri-saturated triacylglycerols obtained when cooled at −25 °C min^{-1} and reheated at 5 °C min $^{-1}$. The polymorphic transitions are reported (Exo up).

(a) Monoacid tri-saturated TAGs (PPP, MMM, and LaLaLa).

In the investigated conditions (cooling −25 °C min^{-1}; reheating 5 °C min^{-1}), PPP is solidified in α-2L (d = 47 Å), which is transformed to the β′-2L (d = 43 Å) and β-2L (d = 41.5 Å) forms upon heating. Final melting is observed at about 66 °C (T_{peak} max) in the β-2 form [23,24] (Figure 2a). MMM crystallized first in α-2L (d = 41 Å), which is transformed to the β′-2L (d = 37 Å) and β-2L (d = 36 Å) forms upon heating, with a final melting at about 57 °C (T_{peak} max) (Figure 2b). Under fast cooling, LaLaLa crystallized first in a very unstable α-2L form (d = 35 Å), which is transformed in the solid state to β-2L (d = 31.4 Å) before final melting at 47 °C (T_{peak} max) (Figure 2c). These three TAGs exhibit the three typical polymorphs of tri-saturated TAGs—α, β′, and β—all under the double chain length structure (2L). In general, 2L structures are observed when the chemical structures of the three fatty acids are the same or very similar [26].

(b) Mixed acid tri-saturated TAGs (MMLa and LaLaM).

A higher complexity in the polymorphic behavior compared to monoacid TAGs has been detected for MMLa and LaLaM. This is linked to the effect of chain-length mismatch.

Under the investigated conditions (cooling −25 °C min^{-1}; reheating 5 °C min^{-1}), LaLaM is also solidified in α-2L (d = 38 Å), followed by a transformation into β′-2L (d = 34.7 Å), which in turns transforms into β-2 2L (d = 34.5 Å), before recrystallization into β-1 2L (d = 33.6 Å); final melting in β-1 is observed at 41 °C (Figure 2d).

Regarding MMLa, it solidifies first in α-2L (d = 39 Å) and then transforms into β′-2 2L (d = 37 Å) then β′-1 2L (d = 35.7 Å) upon heating, with a final melting observed at about 43 °C. No β-form was observed under the investigated conditions (Figure 2e). The heterogeneity of the chain lengths has reduced the differences in the stability between β-prime and β, with the consequence that the β-form is not observed in this case. There are sub-modifications at the β-prime level. In the case of MMLa, two different sub-β′ forms

were observed. The possible existence of multiple β′ forms for saturated TAGs has already been suggested by Hagemann et al. [27,28].

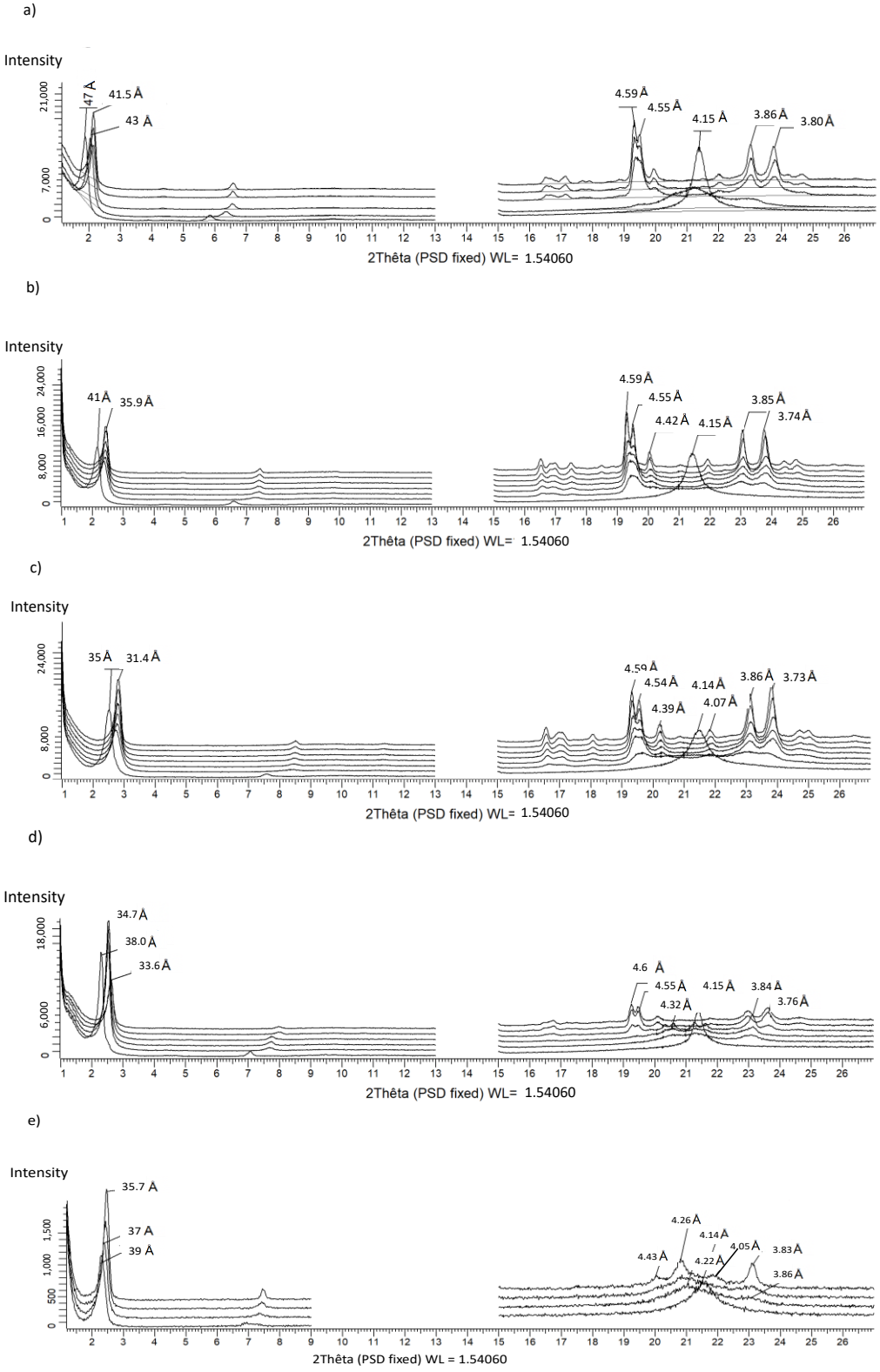

Figure 2. PXRD data of (**a**) PPP and (**b**) MMM and (**c**) LaLaLa and (**d**) LaLaM and (**e**) MMLa; all obtained during the reheating when cooled at −25 °C min^{-1} and reheated at 5 °C min^{-1}.

3.2. Binary Phase Diagrams

All the kinetics binary phase diagrams were built using all the data obtained in the DSC heating thermograms and the corresponding powder XRD data (only some selected PXRD data are shown). The circles in the diagrams represent melting (bold lines), while the squares are related to transitions (dashed lines).

3.2.1. LaLaLa/MMM (Figure 3)

Under the investigated conditions, LaLaLa and MMM, which differ only by two carbons (2C), are miscible in the unstable α-form; one single peak is observed in the short spacing region and in the long spacing region. This behavior is linked to the small difference in carbon chain length (Δ = 2C), as previously reported by Takeuchi et al. [22].

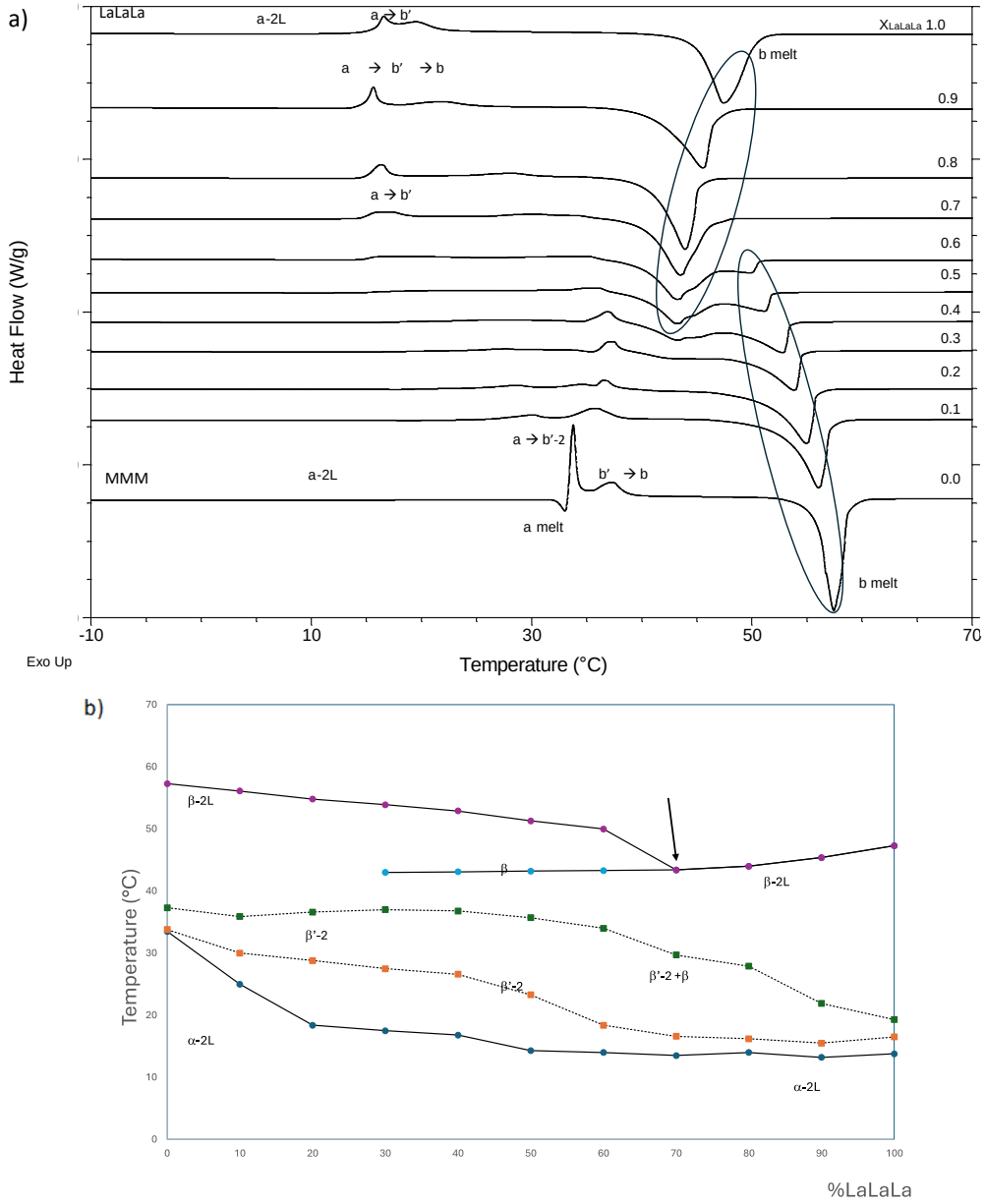

Figure 3. (**a**) DSC melting thermograms of the binary blend LaLaLa–MMM obtained when cooled at −25 °C min^{-1} and reheated at 5 °C min^{-1}. The polymorphic transitions are reported. Mass fractions are reported on each curve at the right-hand side of the figure. (**b**) Kinetic phase behavior diagram of the LaLaLa–MMM binary system constructed using the melting and transition temperatures obtained during reheating at 5 °C min^{-1}. The arrow indicates the eutectic.

Upon heating, a transition from the α-form to the β′-form is observed. Afterwards, both LaLaLa and MMM β forms are observed, forming a eutectic system before final melting. The eutectic point is observed at X_{LaLaLa} = 0.7.

3.2.2. LaLaLa/MMLa (Figure 4)

This second system resembles the previous one, except that one lauric acid (La) replaces one myristic (M) acid, giving rise to a mixed TAG that has a different polymorphic stability. This binary mixture also presents a miscibility in the α form. During heating, the α form is transformed into the β′ form. The behavior of this binary system was greatly dependent on the concentration. Indeed, the stable form of trilaurin is β, but when mixed with MMLa, whose stable form is β′, the mixture presented different stabilities (Figure 4a–c). For blends with X_{LaLaLa} > 0.5, the most stable form was β, while blends with X_{LaLaLa} < 0.5 were strongly affected by the presence of MMLa. For those mixtures, the α form first transforms into the β′-2 form, which, in turns, evolves into a more stable β′-1 form; they finally melted under the β′ form without any β. This binary system also shows an apparent typical eutectic behavior, with a eutectic point being observed at X_{LaLaLa} = 0.5.

a)

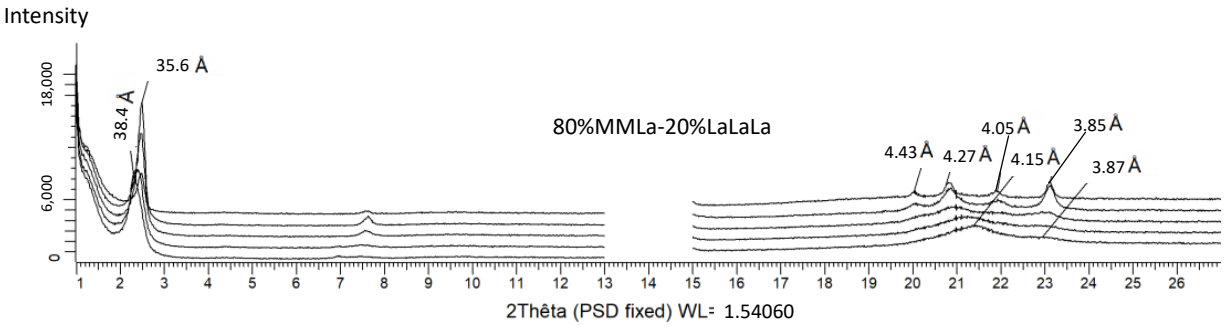

b)

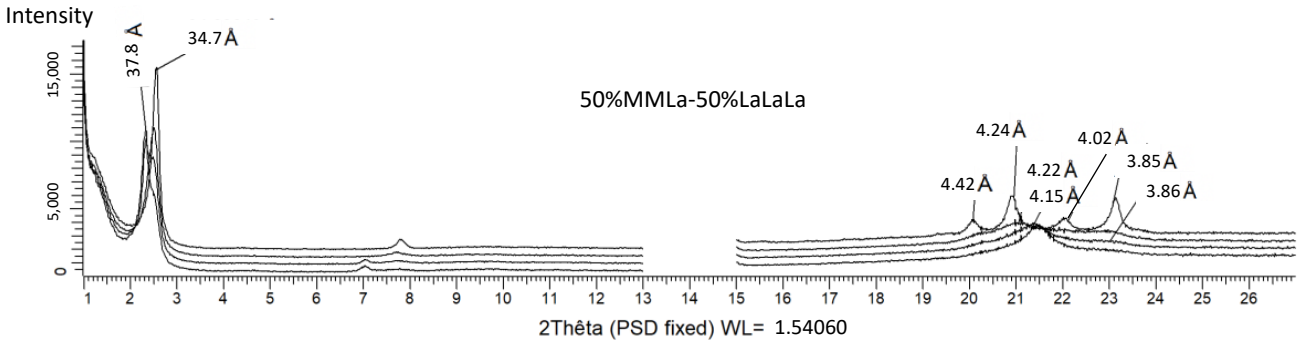

Figure 4. *Cont.*

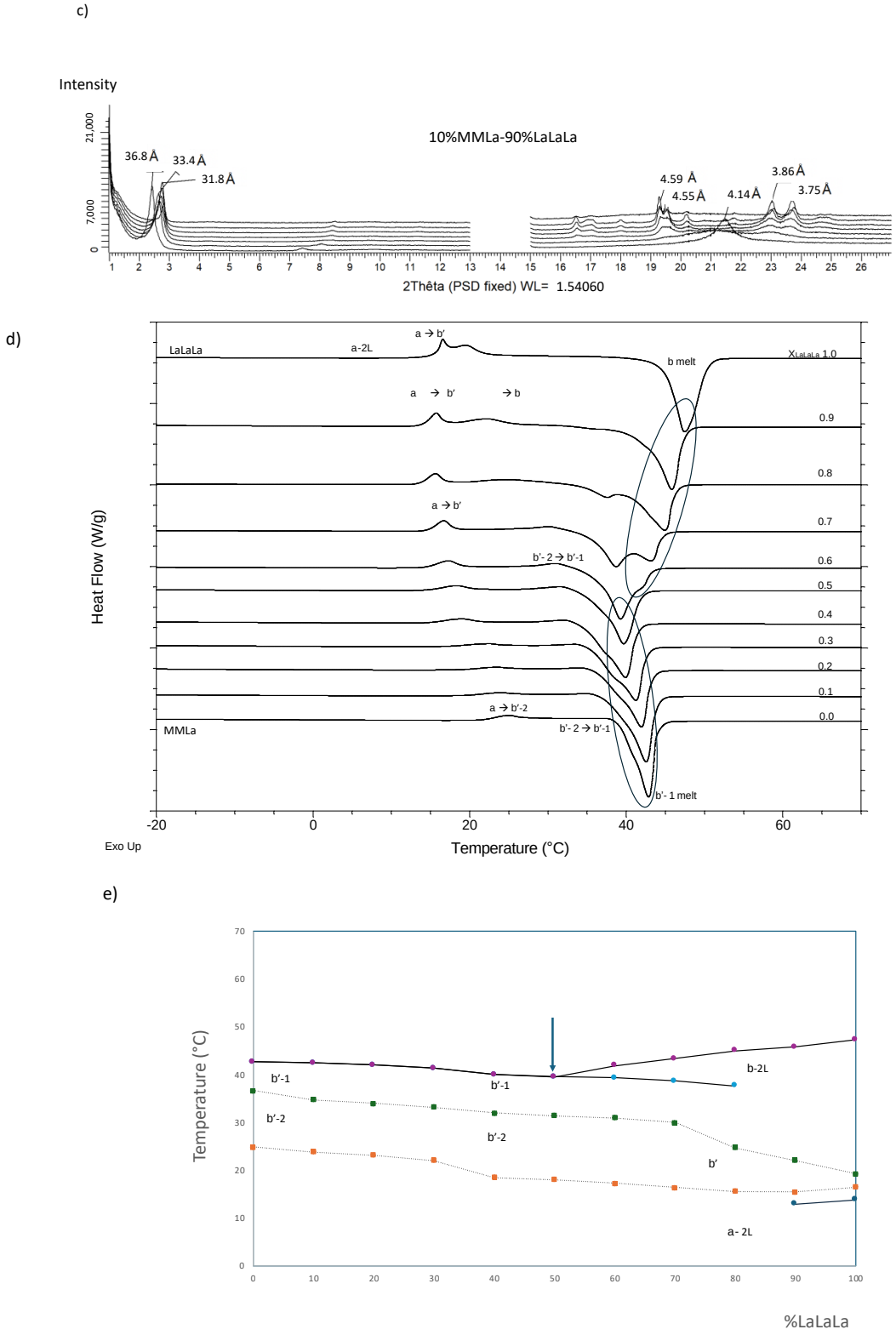

Figure 4. (**a**–**c**) PXRD data of three MMLa–LaLaLa binary blends obtained during the reheating when cooled at −25 °C min^{-1} and reheated at 5 °C min^{-1}; (**d**) DSC melting thermograms of the binary blend LaLaLa–MMLa obtained when cooled at −25 °C min^{-1} and reheated at 5 °C min^{-1}. The polymorphic transitions are reported. Mass fractions are reported on each curve at the right-hand side of the figure. (**e**) Kinetic phase behavior diagram of the LaLaLa–MMLa binary system constructed by using the melting and transition temperatures obtained during reheating at 5 °C min^{-1}. The arrow indicates the eutectic.

3.2.3. LaLaLa/LaLaM (Figure 5)

This third system resembles the previous one, except that one more lauric acid (La) replaces one myristic acid (M), giving rise to another mixed TAG. This binary mixture also presents a miscibility in the α form. Upon heating, a transition from the α form to the β′ form is observed. Afterwards, both the LaLaLa and LaLaM β forms are observed, again forming an apparent typical eutectic system. The eutectic point is observed at $X_{LaLaLa} = 0.25$.

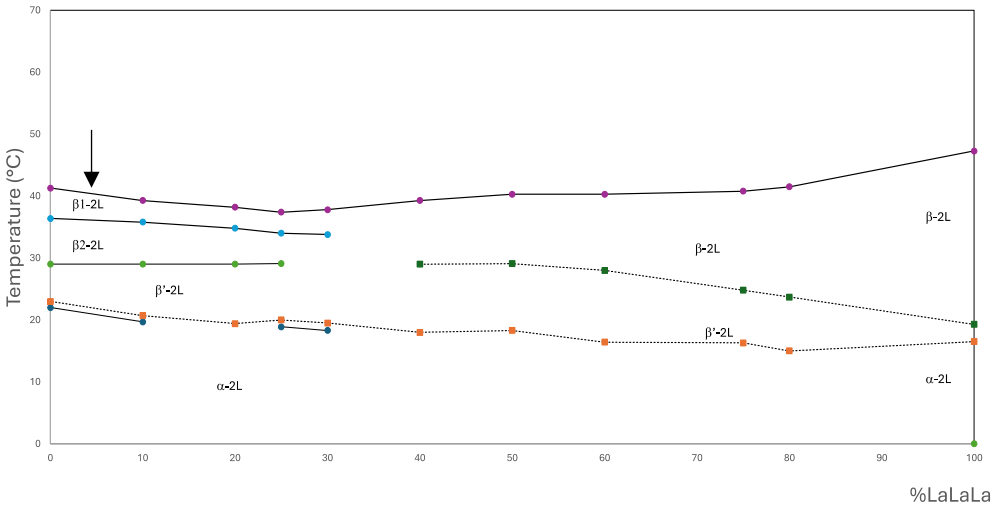

Figure 5. Kinetic phase behavior diagram of LaLaLa–LaLaM binary system constructed using the melting and transition temperatures obtained during reheating at 5 °C min^{-1}. The arrow indicates the eutectic.

3.2.4. MMLa/MMM (Figure 6)

This binary mixture resembles the second one; it also presents a miscibility in the α form. During heating, the α form is first transformed into the β′-2 form, which, in turn, evolves into a more stable β′-1 form for blends made of $X_{MMLa} > 0.4$.

The stable form of MMM is the β form, but when mixed with MMLa, whose stable form is β′, all the mixture with up to $X_{MMM} = 0.4$ melt in the β′ form (Figure 6a). This phase behavior diagram indicates that samples containing lower concentration of MMLa transformed into the most stable β form, like the pure MMM (Figure 6b). A eutectic point is observed at $X_{MMLa} = 0.6$ (Figure 6c), while it was observed at $X_{MMLa} = 0.5$ when mixed with LaLaLa (Figure 4).

a)

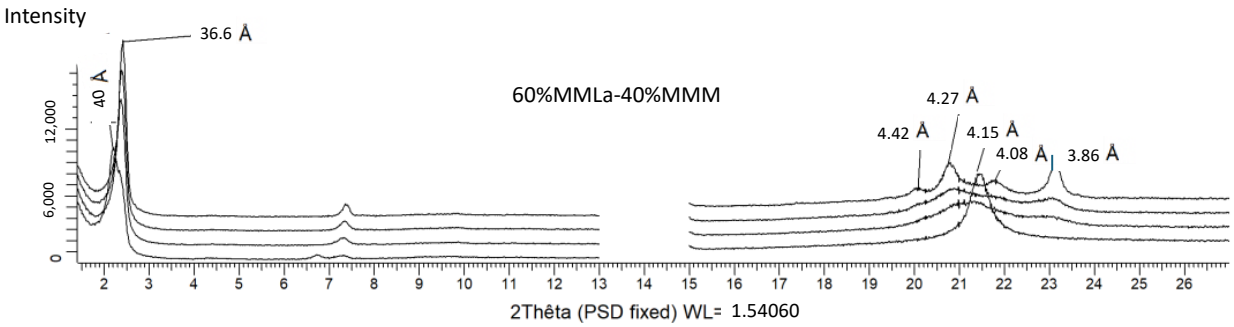

Figure 6. *Cont.*

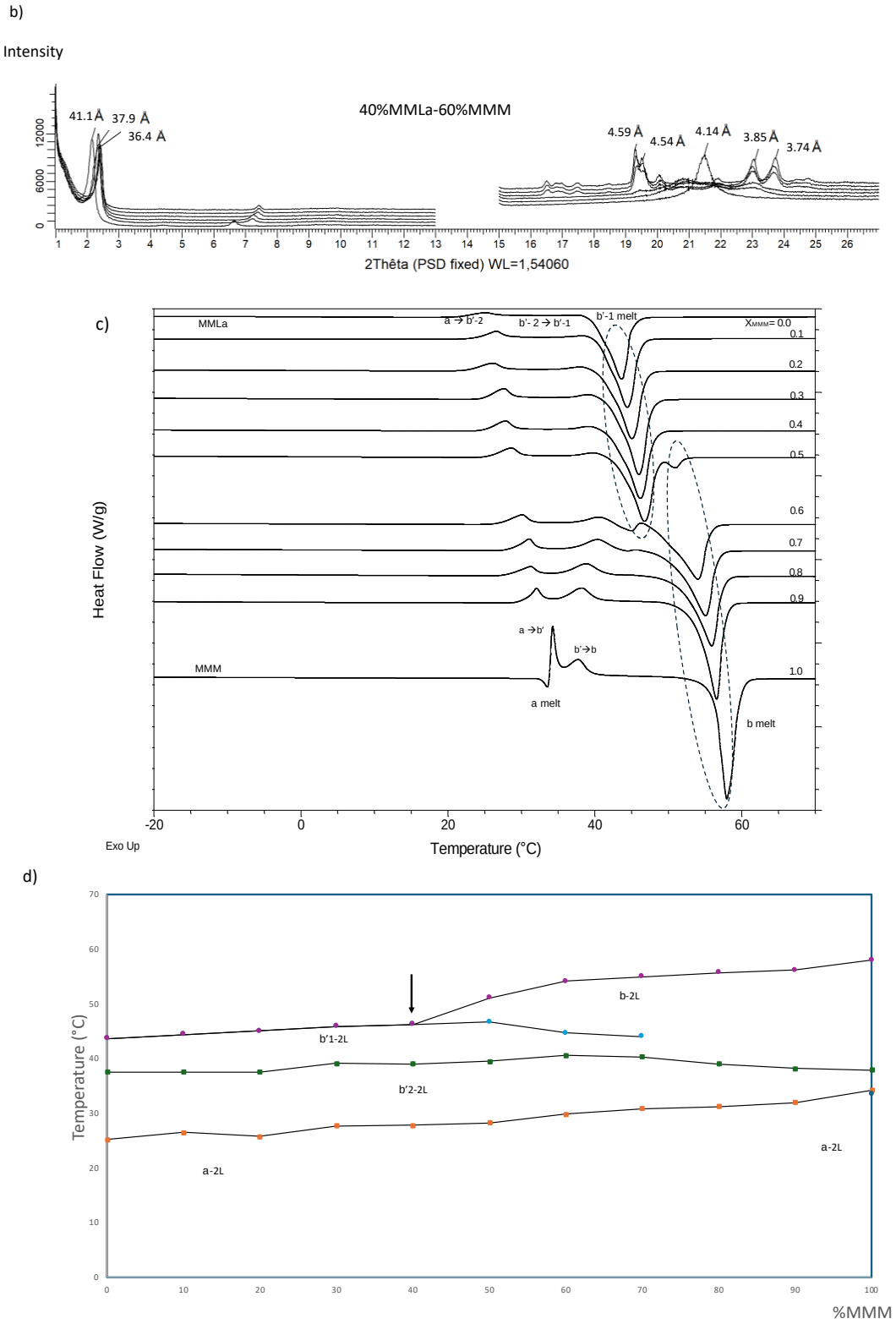

Figure 6. PXRD data of (**a**) 60%MMLa–40%MMM and (**b**) 40%MMLa–60%MMM binary blends obtained during the reheating when cooled at −25 °C.min^{-1} and reheated at 5 °C min^{-1}. (**c**) DSC melting thermograms of the binary blend MMLa–MMM obtained when cooled at −25 °C min^{-1} and reheated at 5 °C min^{-1}. The polymorphic transitions are reported. Mass fractions are reported on each curve at the right-hand side of the figure. (**d**) Kinetic phase behavior diagram of MMLa–MMM binary system constructed using the melting and transition temperatures obtained during reheating at 5 °C min^{-1}. The arrow indicates the eutectic.

3.2.5. LaLaLa–PPP (Figure 7)

Under the investigated conditions, LaLaLa and PPP, which differ by 4C, are not miscible, even in the unstable α form, as already described by Takeuchi et al. [22].

This mixture has different domains, depending on the TAG concentration. The system is also eutectic, with a eutectic point observed at X_{PPP} = 0.1. PPP-rich mixtures all melt under the β form.

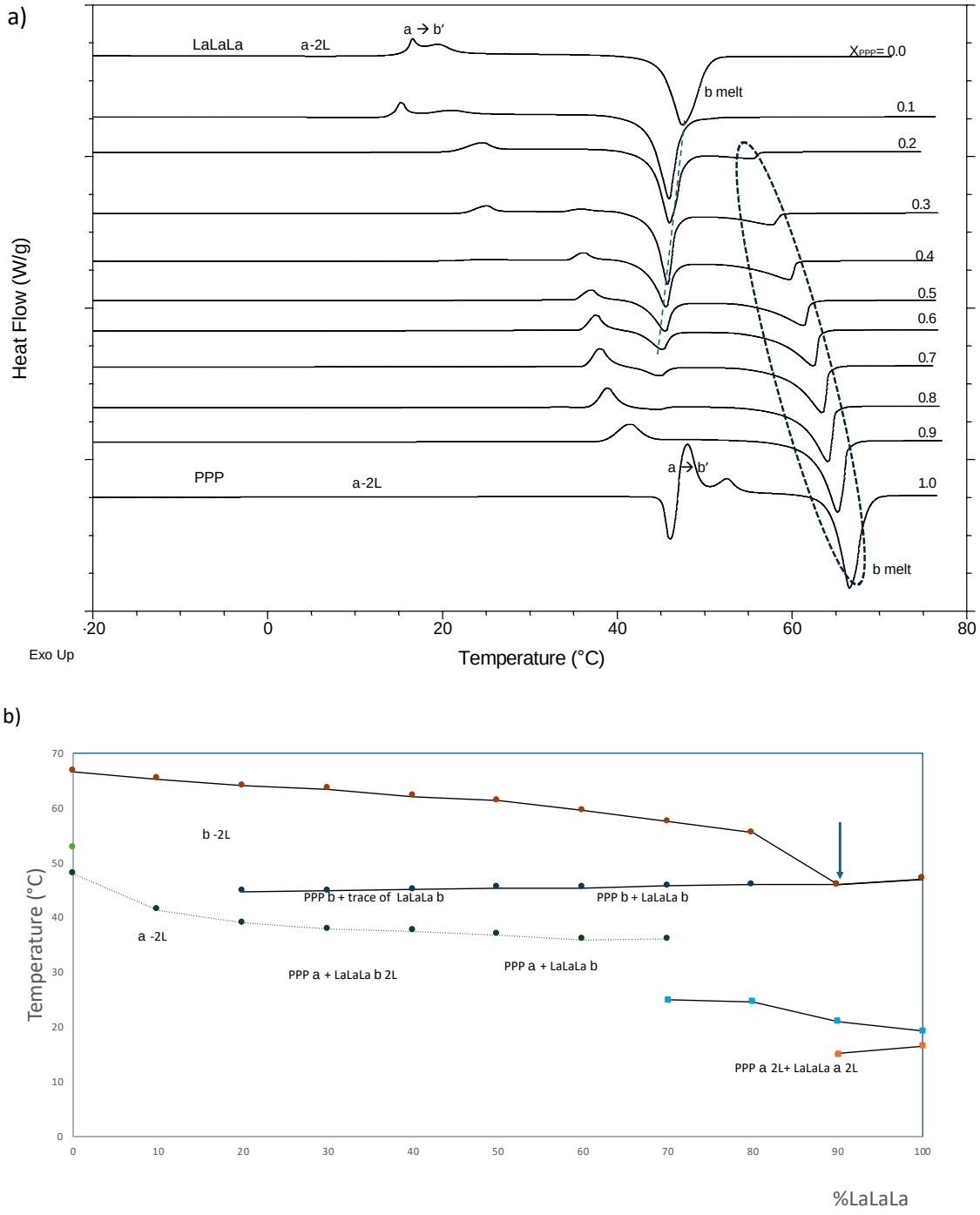

Figure 7. (**a**) DSC melting thermograms of the binary blend LaLaLa–PPP obtained when cooled at −25 °C min^{-1} and reheated at 5 °C min^{-1}. The polymorphic transitions are reported. Mass fractions are reported on each curve at the right-hand side of the figure. (**b**) Kinetic phase behavior diagram of LaLaLa–PPP binary system constructed using the melting and transition temperatures obtained during reheating at 5 °C min^{-1}. The arrow indicates the eutectic.

3.2.6. MMLa/LaLaM (Figure 8)

This binary mixture also presents a miscibility in the α form. During heating, the α form is transformed first into the β′-2 form, which, in turn, evolves into a more stable β′-1 form for blends with $X_{MMLa} > 0.7$. The stable form of LalaM is the β-form, but when mixed with MMLa, whose stable form is β′, all the mixtures with $X_{MMLa} > 0.7$ melt in the β′-1 form. On the contrary, this phase behavior diagram indicates that samples containing lower concentration of MMLa transformed into the most stable β form, like the pure LaLaM.

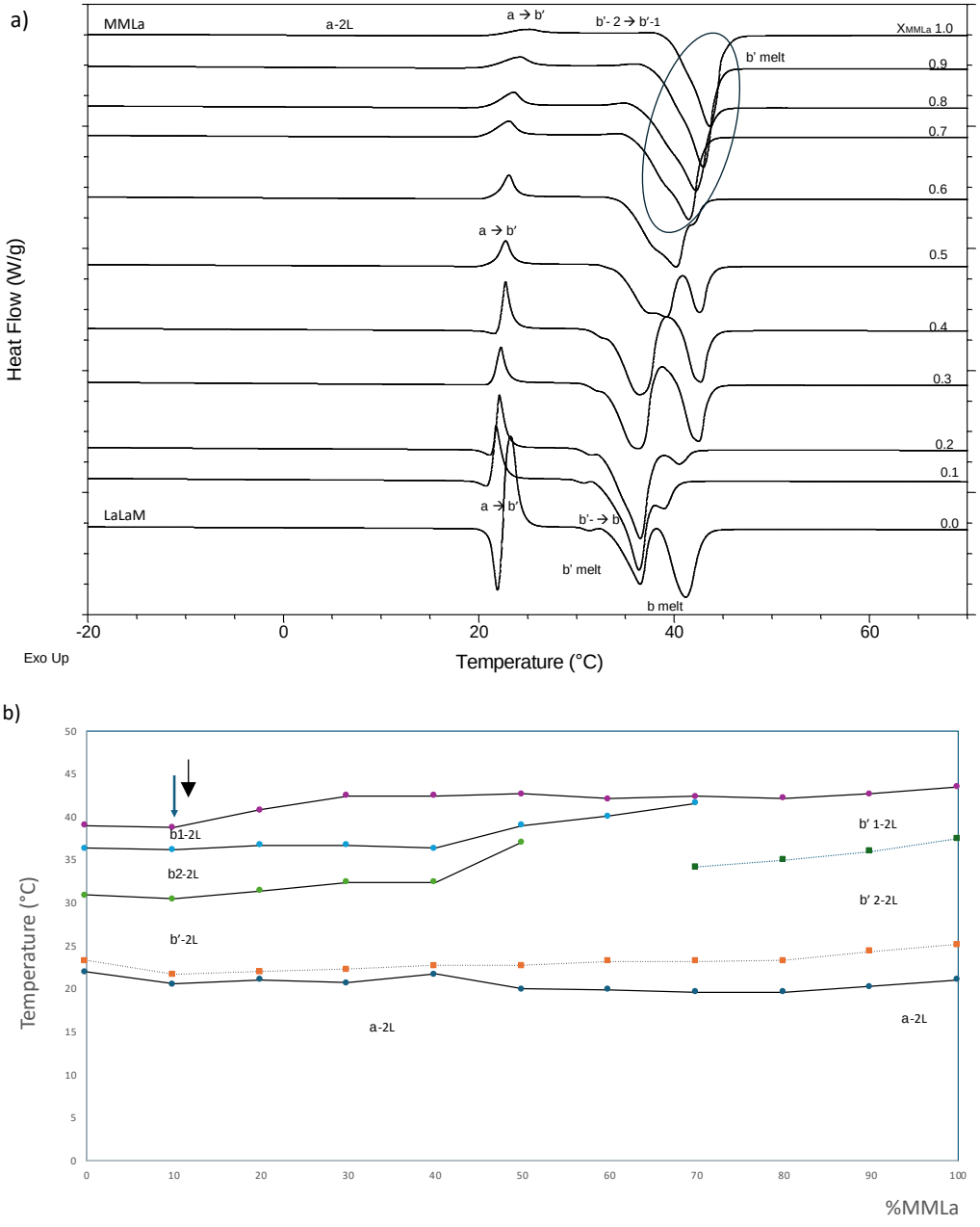

Figure 8. (**a**) DSC melting thermograms of the binary blend MMLa–LaLaM obtained when cooled at −25 °C min^{-1} and reheated at 5 °C min^{-1}. The polymorphic transitions are reported. Mass fractions are reported on each curve at the right-hand side of the figure. (**b**) Kinetic phase behavior diagram of the MMLa–LaLaM binary system constructed using the melting and transition temperatures obtained during reheating at 5 °C min^{-1}. The arrow indicates a eutectic.

4. Conclusions

The kinetic phase behavior of different binary systems all made of tri-saturated TAGs found in typical lauric fats have been investigated thanks to DSC and PXRD techniques.

It was found that all the investigated binary mixtures presented an apparent typical eutectic behavior. The eutectic point varied depending on the blend composition. Introducing mixed saturated TAGs (MMLa or LaLaM) in binary blends led to a shift in the position of the eutectic point. Considering the binary blends made of LaLaLa, it was shifted from X_{LaLaLa} = 0.7 in the LaLaLa–MMM system to X_{LaLaLa} = 0.5 for the LaLaLa–MMLa mixture, and to X_{LaLaLa} = 0.25 for the LaLaLa–LaLaM blend. Finally, the blend made of the two mixed TAGs (MMLa–LaLaM) also presented a complex non-ideal behavior.

Moreover, most of the blends were β-stable. However, the presence of MMLa drastically modified the polymorphic behavior of the blends thereof.

Funding: This research received no external funding.

Data Availability Statement: The original contributions presented in the study are included in the article, further inquiries can be directed to the corresponding author.

Acknowledgments: The author thanks S. Filocco for his technical assistance.

Conflicts of Interest: The author declares no conflicts of interest.

References

1. Yamoneka, J.; Malumba, P.; Blecker, C.; Gindo, M.; Richard, G.; Fauconnier, M.L.; Lognay, G.; Danthine, S. Physicochemical properties and thermal behaviour of African wild mango (*Irvingia gabonensis*) seed fat. *LWT* **2015**, *64*, 989–996. [CrossRef]
2. Anihouvi, A.; Blecker, C.; Dombrée, A.; Danthine, S. Comparative Study of Thermal and Structural Behavior of Four Industrial Lauric Fats. *Food Bioprocess. Technol.* **2013**, *6*, 3381–3391. [CrossRef]
3. Gibon, V. Chapter 12: Palm Oil and Palm Kernel Oil Refining and Fractionation Technology. In *Palm Oil*; AOCS Press: Champaign, IL, USA, 2012; pp. 329–375.
4. Sonwai, S.; Podchong, P.; Rousseau, D. Crystallization Kinetics of Coconut Oil in the Presence of Sorbitan Esters with Different Fatty Acid Moieties. *J. Am. Oil Chem. Soc.* **2016**, *93*, 849–858. [CrossRef]
5. Salas, J.; Bootello, M.; Martinez-Force, E.; Garces, R. Tropical vegetable fats and butters: Properties and new alternatives. *Ol. Corps Gras Lipides* **2009**, *16*, 254–258. [CrossRef]
6. Srisuksai, K.; Limudomporn, P.; Kovitvadhi, U.; Thongsuwan, K.; Imaram, W.; Lertchaiyongphanit, R.; Sareepoch, T.; Kovitvadhi, A.; Fungfuang, W. Physicochemical properties and fatty acid profile of oil extracted from black soldier fly larvae (*Hermetia illucens*). *Vet. World* **2024**, *7*, 518–526. [CrossRef]
7. Tsuiji, H.; Takeuchi, H.; Nakamura, M.; Okazaki, M.; Kondo, K. Dietary medium-chain triacylglycerols suppress accumulation of body fat in a double-blind, controlled trial in healthy men and women. *J. Nutr.* **2001**, *131*, 2853–2859. [CrossRef]
8. Sonwai, S.; Rungprasertphol, P.; Nantipipat, N.; Tungvongcharoan, S.; Laiyangkoon, N. Characterization of Coconut Oil Fractions Obtained from Solvent Fractionation Using Acetone. *J. Oleo Sci.* **2016**, *66*, 951–961. [CrossRef]
9. Maruyama, J.M.; Soares, F.; D'Agostinho, N.R.; Goncalves, M.; Gioielli, L.; da Silva, R.C. Effects of emulsifier addition on the crystallization and melting behavior of palm olein and coconut oil. *J. Agric. Food Chem.* **2014**, *62*, 2253–2263. [CrossRef]
10. Che Man, Y.B.; Shamsi, K.; Yusoff, M.S.A.; Jinap, S. A study on the crystal structure of palm oil-based whipping cream. *J. Am. Oil Chem. Soc.* **2003**, *80*, 409–415. [CrossRef]
11. Md Ali, A.R.; Dimick, P.S. Melting and solidification characteristics of confectionery fats: Anhydrous milk fat, cocoa butter and palm kernel stearin blends. *J. Am. Oil Chem. Soc.* **1994**, *71*, 803–806. [CrossRef]
12. Pantzaris, T.P.; Basiron, Y. The lauric (coconut and palm kernel) oils. In *Vegetable Oils in Food Technology: Composition, Properties and Uses*; Gunstone, F.D., Ed.; Blackwell: Oxford, UK, 2002; pp. 157–202.
13. Tan, C.P.; Che Man, Y.B. Differential scanning calorimetric analysis of edible oils: Comparison of thermal properties and chemical composition. *J. Am. Oil Chem. Soc.* **2000**, *77*, 143–155. [CrossRef]
14. Noordin, M.I.; Chung, L.Y. Thermostability and polymorphism of theobroma oil and palm kernel oil as suppository bases. *J. Therm. Anal. Calorim.* **2009**, *95*, 891–894. [CrossRef]
15. Awad, T.; Sato, K. Acceleration of crystallisation of palm kernel oil in oil-in-water emulsion by hydrophobic emulsifier additives. *Colloids Surf. B Biointerfaces* **2002**, *25*, 45–53. [CrossRef]
16. Cornacchia, L.; Roos, Y.H. Solid–liquid transition and stability of HPKO-in-water systems emulsified by dairy proteins. *Food Biophys.* **2011**, *6*, 288–294. [CrossRef]
17. Cornacchia, L.; Roos, Y.H. Lipid and water crystallization in protein-stabilised oil-in-water emulsions. *Food Hydrocoll.* **2011**, *25*, 1726–1736. [CrossRef]

18. Relkin, P.; Ait-Taleb, A.; Sourdet, S.; Fosseux, P.-Y. Thermal behavior of fat droplet as related to adsorbed milk proteins in complex food emulsions. A DSC study. *J. Am. Oil Chem. Soc.* **2003**, *80*, 741–746. [CrossRef]
19. Relkin, P.; Sourdet, S.; Fosseux, P.-Y. Fat crystallization in complex food emulsions. Effects of adsorbed milk proteins and of a whipping process. *J. Therm. Anal. Calorim.* **2003**, *71*, 187–195. [CrossRef]
20. Relkin, P.; Sourdet, S. Factors affecting fat droplet aggregation in whipped frozen protein-stabilized emulsions. *Food Hydrocoll.* **2005**, *19*, 503–511. [CrossRef]
21. Gibon, V.; Danthine, S. Systematic Investigation of Co-Crystallization Properties in Binary and Ternary Mixtures of Triacylglycerols Containing Palmitic and Oleic Acids in Relation with Palm Oil Dry Fractionation. *Foods* **2020**, *9*, 1891. [CrossRef]
22. Takeuchi, M.; Ueno, S.; Sato, K. Synchrotron Radiation SAXS/WAXS Study of Polymorph-Dependent Phase Behavior of Binary Mixtures of Saturated Monoacid Triacylglycerols. *Cryst. Growth Des.* **2003**, *3*, 369–374. [CrossRef]
23. Macridachis-Gonzales, J.; Bayes-Garcia, L.; Calvet, T. An Insight into the Solid-State Miscibility of Triacylglycerol Crystals. *Molecules* **2020**, *25*, 4562. [CrossRef] [PubMed]
24. Bhaggan, K.; Smith, K.; Blecker, C.; Danthine, S. Binary Mixtures of Tripalmitoylglycerol (PPP) and 1,3-Dipalmitoyl-2-stearoyl-sn-glycerol (PSP): Polymorphism and Kinetic Phase Behavior. *Eur. J. Lipid Sci. Technol.* **2018**, *120*, 1700306. [CrossRef]
25. Bhaggan, K.; Smith, K.; Blecker, C.; Danthine, S. Polymorphism and Kinetic Behavior of Binary Mixtures of Trisaturated Triacylglycerols Containing Palmitic and Stearic Acid Under Non-Isothermal Conditions. *Eur. J. Lipid Sci. Technol.* **2018**, *120*, 1800072. [CrossRef]
26. Himawan, C.; Starov, V.M.; Stapley, A.G.F. Thermodynamic and kinetic aspects of fat crystallization. *Adv. Colloid Interface Sci.* **2006**, *122*, 3–33. [CrossRef]
27. Takeguchi, S.; Sato, A.; Hondoh, H.; Uehara, H.; Ueno, S. Multiple β Forms of Saturated Monoacid Triacylglycerol Crystals. *Molecules* **2020**, *25*, 5086. [CrossRef]
28. Hagemann, J.W.; Tallent, W.H.; Kolb, K.E. Differential scanning calorimetry of single acid triglycerides: Effect of chain length and unsaturation. *J. Am. Oil Chem. Soc.* **1972**, *49*, 118–123. [CrossRef]